

Phase imaging and the lever-sample tilt angle in dynamic atomic force microscopy

Matthew J. D'Amato

Materials Science Program, University of Wisconsin, Madison, Wisconsin 53706

Matthew S. Marcus and Mark A. Eriksson

Department of Physics, University of Wisconsin, Madison, Wisconsin 53706

Robert W. Carpick^{a)}

Department of Engineering Physics, University of Wisconsin, Madison, Wisconsin 53706

(Received 5 January 2004; accepted 2 September 2004)

The phase shift in amplitude-controlled dynamic atomic force microscopy (AFM) is shown to depend on the cantilever-sample tilt angle. For a silicon sample and tip the phase shift changes by nearly 15° for a change in tilt angle of 15° . This contribution to the phase results from the oscillating tip's motion parallel to the surface, which contributes to the overall energy dissipation. It occurs even when the measurements are carried out in the attractive regime. An off-axis dynamic AFM model incorporating van der Waals attraction and a thin viscous damping layer near the surface successfully describes the observed phase shifts. This effect must be considered to interpret phase images quantitatively. © 2004 American Institute of Physics. [DOI: 10.1063/1.1812839]

Atomic force microscopy (AFM) is widely used to measure topography and other surface or interfacial properties including friction, adhesion, and elasticity with high spatial resolution. Dynamic AFM is a mode of operation in which the probe is oscillated as it is scanned.¹ What is commonly referred to as intermittent-contact, tapping mode, or amplitude-modulated AFM all refer to a specific type of dynamic AFM in which the amplitude is held constant. This work is obtained in this mode.² Dynamic AFM was first established to enhance spatial resolution and enable imaging of fragile samples. It is particularly well suited to the imaging of soft and biological materials since it avoids shear forces and limits tip-sample interactions.³ Furthermore, the phase shift between the drive and response signals is easily measured, and is a sensitive probe of tip-sample interactions. It is increasingly used to image qualitative differences in sample composition with high spatial resolution.^{4,5} However, the *quantitative* interpretation of phase data remains extremely challenging due to the significant number of parameters which contribute to the contrast.

Several models have been developed to describe the nature of the phase contrast and have demonstrated its dependence on multiple factors, including tip and sample elasticity/viscoelasticity, adhesion and other surface forces, and tip size and shape.^{6–9} Work by Burnham *et al.* describes a full solution, including Maugis mechanics, of dynamic AFM.⁶ García and San Paulo have emphasized that there are two stable regimes of dynamic AFM, one involving purely attractive forces and one that also involves repulsive forces.¹⁰ Cleveland *et al.* have shown that the phase shift is related to the power dissipated in the tip-sample interaction provided the tip motion is nearly sinusoidal.¹¹ In all of these models, tip-sample interactions are considered as purely out-of-plane phenomena (i.e., with forces and displacements along the surface normal). A contribution to phase contrast was recently discovered by Marcus *et al.*, who showed that

quantitative phase imaging is sensitive to the in-plane structural anisotropy in a polymer thin film.¹² This arises from the fact that the cantilever is tilted with respect to the sample by $10\text{--}15^\circ$ in many instruments. Most recently, the effect of cantilever tilt was addressed by Heim, Kappl, and Butt who consider its effects on the spring constant and adhesion measurements in contact mode.¹³ As some amount of tilt is universal in AFM design, it is desirable to understand its effect on the measured phase. This would enable the effect of topography on phase measurements to be unraveled—an important issue for interpreting phase images quantitatively.

We perform an experiment to measure the correlation of the cantilever-sample tilt angle with the phase shift. The experiment is carried out entirely in the attractive regime. A model incorporating van der Waals attraction is developed with resolved normal and in-plane viscous damping terms to describe our data. Our inclusion of the effect of the lever-sample tilt allows us to deconvolute tilt-induced phase shifts.

Two small wedges are machined with angles of 5 and 10° of tilt. Mounting samples on these wedges allows for relative lever-sample tilt angles of 6 , 11 , 16 , and 21° (see Fig. 1). Silicon (111) wafers are cut and glued to both the standard mounting disks as well as the wedges which are in turn glued to the disks. No particular sample preparation is made—the silicon wafers have a native oxide surface layer. No data could be obtained for 1° tilt due to the proximity of the cantilever beam to the sample. Regions of $1\text{--}2\ \mu\text{m}^2$ are imaged at a scan rate of $1\ \text{Hz}$, and the relatively constant phase (less than 1° rms variation) over very flat regions (typically less than $0.2\ \text{nm}$ rms roughness) is averaged.¹⁴ Tilt angles are used in random order to ensure reproducibility and to decouple any systematic effects such as drift. Data are collected for three scans at a time. The data are averaged

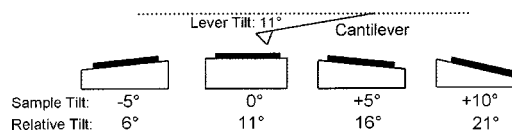


FIG. 1. Geometry of cantilever and samples.

^{a)} Author to whom correspondence should be addressed; electronic mail: carpick@engr.wisc.edu

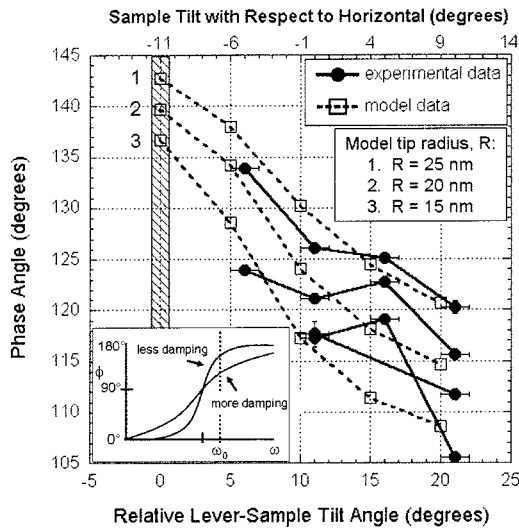


FIG. 2. Experimental data (circles) and results from our model (squares) are shown. All data are acquired with the same set point. Offsets between experiments are attributed to variations in the tips and environmental conditions. Vertical error bars of $\pm 1^\circ$ are reported. Model is for a work of adhesion $\gamma=0.125$ J/m², damping layer thickness 0.5 nm, normal quality factor 10, and lateral quality factor 0.1. The three model curves correspond to the tip radii as shown. Decrease in phase angle with increased damping.

together to produce the plot shown in Fig. 2. For some experiments, data for all four tilt angles could not be acquired due to tip crashes or instrumental limitations. All other experimental parameters are given as a reference.^{15,16}

From the data in Fig. 2, there is a clear decreasing trend towards 90° with increasing positive tilt. As much as a 15° change in phase is observed for a 15° change in lever-sample tilt. In four runs of the same experiment (with four different cantilevers and laser alignments), the results show the same trend. The free amplitude was neither reset nor drifted significantly during any one experiment, which means the phase could not have shifted artificially. We attribute offsets in the data to variable tip properties (such as tip radius and surface chemistry) and environmental conditions. In fact, these variations can be reproduced by our model (described below) by changing the tip radius or tip-sample adhesion energy, for example. If we are interested in the case where the cantilever oscillates normal to the surface (corresponding to all previous models of dynamic AFM), then we must extrapolate the data to -11° of sample tilt (shaded region in Fig. 2). For the measurements performed here, the absolute value of the

$$\ddot{p} + \frac{\omega_0}{Q_{\text{cant}}}(\dot{p} - \dot{\xi}) + \omega_0^2(p - \xi) = \begin{cases} \frac{\omega_0^2}{k} \left(\frac{AR \cos \psi}{6(p \cos \psi - \xi_0)^2} \right) & p \geq 0.5 \text{ nm} \\ \frac{\omega_0^2}{k} \left(\frac{AR \cos \psi}{6(p \cos \psi - \xi_0)^2} \right) - \frac{\omega_0}{Q_{\text{norm}}} \dot{p} \cos^2 \psi - \frac{\omega_0}{Q_{\text{lat}}} \dot{p} \sin^2 \psi & 0 < p < 0.5 \text{ nm} \\ -\cos \psi (K \sqrt{R} p^{3/2} \cos^{3/2} \psi - 2\pi \gamma R) & p \leq 0 \text{ nm} \end{cases} \quad (1)$$

where p is the position of the tip above the sample along the axis perpendicular to the cantilever base, ξ is the position of the cantilever base, Q_{cant} , ω_0 , and k are the quality factor, resonance frequency and spring constant of the cantilever, Q_{norm} and Q_{lat} are normal and lateral quality factors for

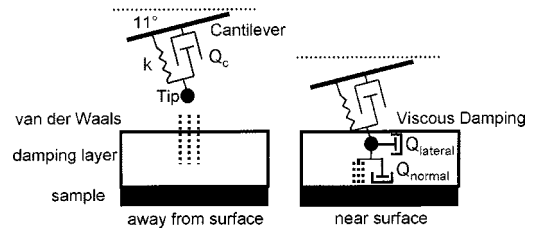


FIG. 3. The tip-sample interaction in the attractive regime. This model, based on a van der Waals interaction (dashed lines), includes a thin (0.5 nm) damping layer. Not shown is the repulsive interaction from DMT contact mechanics.

phase is always above 90° . This corresponds to the case where the tip-sample interaction is dominated by attractive forces.¹⁰ Preliminary measurements indicate that a corresponding trend is also seen for phase shifts below 90° , i.e., for repulsive tip-sample interactions. This makes sense because the increase in lateral damping with tilt broadens the phase resonance curve (see inset in Fig. 2) and thus shifts the phase towards 90° at our drive frequency, which is slightly greater than the near-surface resonance frequency.

To model the tip-sample interaction we begin with a sinusoidally driven, damped harmonic oscillator. The tip is assumed to be a point mass and is constrained to move along the direction normal to the cantilever base (see Fig. 3). Tip-sample forces are resolved into in-plane and normal components with respect to the surface. The tip interacts with the surface via the van der Waals force and is modeled as a sphere approaching a plane. An adhesive contact mechanics model is used to match the van der Waals force with the adhesion force.^{17–19} From this mechanics analysis the work of adhesion γ , the equilibrium separation ξ_0 , and the Hamaker constant A , become dependent on each other: $\gamma = A/12\pi\xi_0^2$. Adjusting any of these in our model has the same effect: altering the strength of the van der Waals interaction. In addition, the tip radius, R , is directly proportional to the strength of the van der Waals term. Therefore, we choose to vary only R in our model as shown, with physically reasonable values for all other parameters.²⁰ Our model is capable of simulating steady-state imaging conditions in either the repulsive or attractive regimes, consistent with the results of García and San Paulo.¹⁰ Our experiments were carried out in the attractive regime, and consistent with this, our model exhibits repulsive interactions only transiently at the outset of each simulation.

Newton's equation of motion in this model becomes

damping near the surface, K is the reduced contact modulus between tip and sample, and ψ is the relative lever-sample tilt angle. Equation (1) is solved numerically using the MATLAB® differential equation solver ODE113 (The MathWorks, Inc., Natick, MA) and the phase is extracted using a

Fourier transform of the position as a function of time.

The last two terms in Eq. (1) for values of p within 0.5 nm of the surface represent the effect of a thin viscous damping layer. These damping forces are the only terms that dissipate energy in the attractive regime ($p > 0$) and thus change the phase significantly as the tilt is varied. While in-plane dissipation could be explained in repulsive steady-state conditions by the effect of interfacial friction, we find it surprising that the phase changes significantly while the tip remains in the *attractive* regime. This is true for all experimental data presented here, where phase angles are greater than 90° (repulsive forces are not contributing to the tip-sample interaction in the steady state and this necessitates the inclusion of a near-surface in-plane dissipative effect). Therefore, the interactions are dominated purely by the van der Waals interaction, and, in our model, the viscous damping layer. The damping layer is chosen to have a thickness of 0.5 nm here although this number is by no means uniquely determined. However, we consider it to be physically reasonable. Our model predicts the phase shifts as shown in Fig. 2 with Q_{norm} and Q_{lat} of 10 and 0.1, respectively. Adjusting Q_{norm} or any of the parameters relating to the strength of the van der Waals interaction (γ, ξ_0, R, A) shifts the entire phase versus tilt curve vertically, but does not alter the *variation* in phase with tilt angle over the given range of tilts (the slope of the data). This is illustrated in Fig. 2 for the case of varying R . The left side of Eq. (1) contains a quality factor for the cantilever which includes air damping effects. However, adjusting Q_{cant} has a negligible effect on the change in phase shift with sample tilt compared to that observed in the experiment. Only Q_{lat} adjusts the change in phase with sample tilt, and it must be approximately 0.1 (corresponding to very strong damping) to reproduce our experimental slope.

Physically, the thin viscous damping layer could describe a contamination layer just above the Si surface (water layer, hydrocarbon layer, or otherwise). Future experiments performed in ultrahigh vacuum could yield information about the influence of the surface layer. Strongly separation-dependent air damping between the cantilever/tip and the sample could also be a contributing factor. Future improvements could include more sophisticated descriptions of the cantilever mechanics, the contact mechanics (to include Maugis' mechanics as Burnham has done⁶) and the viscous layer.

Cleveland *et al.* have shown that the average power dissipated due to the tip-sample interaction is well described by

$$\bar{P}_{\text{tip}} = \frac{1}{2} \frac{kA^2 \omega_0}{Q_{\text{cant}}} \left[\left(\frac{A}{A_0} \right) \sin \phi - 1 \right], \quad (2)$$

where A_0 is the free amplitude of oscillation, A is the amplitude during imaging, and ϕ is the phase of the oscillation relative to the drive amplitude.¹¹ Equation (2) is independent of the energy dissipation mechanism, provided the tip's motion is nearly sinusoidal, as it is in our experiment. Thus, the variations in phase we observe indicate variations in the dissipated power. Because the overall phase in Fig. 2 is larger than 90° , and the amplitude was held constant, an increase in ϕ corresponds to a decrease in the power dissipated. Thus, the power dissipated is at a minimum when the net lever-sample tilt angle (and thus the in-plane dissipation) is minimized. From Eq. (2), with a 15° change in local tilt angle, we

predict nearly a 15% change in power dissipated. This is a significant effect and cannot be ignored when interpreting phase measurements. As well, it indicates that local slopes on a sample due to topography may induce a phase shift even if the material is completely homogeneous.

In summary, we present quantitative phase measurements in the attractive regime of amplitude-controlled dynamic AFM, understood with a force interaction model that includes a thin viscous damping layer. Resolved normal and lateral quality factors describe a high amount of damping whose effect varies with the relative lever-sample tilt angle and matches the experimental data. This effect can now be described and should be accounted for in quantitative interpretations of phase images in dynamic AFM.

The authors acknowledge funding from the NSF CAREER program, Grant No. DMR0094063 (M.A.E.) and Grant No. CMS0134571 (R.W.C.), the Research Corporation (M.A.E.), the NSF MRSEC program Grant No. DMR0079983, and the University of Wisconsin-Madison.

¹Y. Martin, C. C. Williams, and H. K. Wickramasinghe, *J. Appl. Phys.* **61**, 4723 (1987).

²For brevity, amplitude-controlled dynamic AFM is referred to simply as dynamic AFM throughout this letter.

³A. Engel, H. E. Gaub, and D. J. Müller, *Curr. Biol.* **9**, R133 (1999).

⁴D. Chernoff, *Proc. Microsc. Microanal.*, MSA (Jones and Begell, New York, 1995), Vol. 888.

⁵R. García and R. Pérez, *Surf. Sci. Rep.* **47**, 197 (2002).

⁶N. A. Burnham, O. P. Behrend, F. Oulevey, G. Gremaud, P.-J. Gallo, D. Gourdon, E. Dupas, A. J. Kulik, H. M. Pollock, and G. A. D. Briggs, *Nanotechnology* **8**, 67 (1997).

⁷O. P. Behrend, F. Oulevey, D. Gourdon, E. Dupas, A. J. Kulik, G. Gremaud, and N. A. Burnham, *Appl. Phys. A: Mater. Sci. Process.* **66**, S219 (1998).

⁸J. P. Aimé, R. Boisgard, L. Nony, and G. Couturier, *J. Chem. Phys.* **114**, 4945 (2001).

⁹J. Tamayo and R. García, *Langmuir* **12**, 4430 (1996).

¹⁰R. García and A. San Paulo, *Phys. Rev. B* **60**, 4961 (1999).

¹¹J. P. Cleveland, B. Anczykowski, A. E. Schmid, and V. B. Elings, *Appl. Phys. Lett.* **72**, 2613 (1998).

¹²M. S. Marcus, R. W. Carpick, D. Y. Sasaki, and M. A. Eriksson, *Phys. Rev. Lett.* **88**, 226103 (2002).

¹³L.-O. Heim, M. Kappl, and H.-J. Butt, *Langmuir* **20**, 2760 (2004).

¹⁴The reported phase shifts are true phase shifts with respect to the drive signal. Phase shifts reported by the instrument are not properly scaled and are shifted by 90° .

¹⁵All phase images are acquired with a Digital Instruments MultiMode SPM and Nanoscope IIIa controller, using Si cantilevers in ambient laboratory conditions. The free amplitude $A_0 = 10.5$ nm, cantilever quality factor $Q_{\text{cant}} = 400$, resonance frequency $\omega_0 = 2\pi \times 265$ kHz, and damped (set point) amplitude $A = 5.25$ nm are all measurable with or controlled by the AFM controller. For all experiments, the cantilever is driven at the resonance frequency measured far from the sample, which is slightly higher than the resonance frequency during imaging due to the tip's interaction with the surface. An average value for the cantilever spring constant of 25 N/m is measured using the method of Sader and co-workers (Ref. 16).

¹⁶J. E. Sader, J. W. M. Chon, and P. Mulvaney, *Rev. Sci. Instrum.* **70**, 3967 (1999).

¹⁷The correct adhesive contact mechanics model to use depends on the value of Tabor's parameter, which we have estimated for our system (Ref. 18). Based on this, we choose the Derjaguin-Müller-Toporov (DMT) model (Ref. 19).

¹⁸D. Tabor, *J. Colloid Interface Sci.* **58**, 2 (1977).

¹⁹B. V. Derjaguin, V. M. Müller, and Y. P. Toporov, *J. Colloid Interface Sci.* **53**, 314 (1975).

²⁰Measured values for the pull-off force (40–60 nN) are obtained from force-distance curves. Substituting these values into the DMT model, we obtain a range for the values of γ (150–180 J/m²) using a tip radius of 30 nm.